HHS Public Access

Author manuscript

J Prosthodont. Author manuscript; available in PMC 2016 February 26.

Published in final edited form as:

J Prosthodont. 2016 February ; 25(2): 105–115. doi:10.1111/jopr.12316.

Gingival Mesenchymal Stem Cell (GMSC) Delivery System Based on RGD-Coupled Alginate Hydrogel with Antimicrobial Properties: A Novel Treatment Modality for Peri-Implantitis

Ivana M. A. Diniz, DDS, MSc[1,2], **Chider Chen, PhD**[3], **Sahar Ansari, PhD**[1,4], **Homayoun H. Zadeh, DDS, PhD**[4], **Maryam Moshaverinia, DDS, MSc**[5], **Daniel Chee**[1], **Márcia M. Marques, DDS, PhD**[2], **Songtao Shi, DDS, PhD**[3], and **Alireza Moshaverinia, DDS, MS, PhD, FACP**[1]

[1]Center for Craniofacial Molecular Biology, Ostrow School of Dentistry of USC, University of Southern California, Los Angeles, CA

[2]Restorative Dentistry Department, School of Dentistry, Universidade de São Paulo, São Paulo, Brazil

[3]Department of Anatomy and Cell Biology, School of Dental Medicine, University of Pennsylvania

[4]Laboratory for Immunoregulation and Tissue Engineering (LITE), Ostrow School of Dentistry of USC, University of Southern California, Los Angeles, CA

[5]Department of Oral and Maxillofacial Medicine, School of Dentistry, Shiraz University of Medical Sciences, Shiraz, Iran

Abstract

Purpose—Peri-implantitis is one of the most common inflammatory complications in dental implantology. Similar to periodontitis, in peri-implantitis, destructive inflammatory changes take place in the tissues surrounding a dental implant. Bacterial flora at the failing implant sites resemble the pathogens in periodontal disease and consist of Gram-negative anaerobic bacteria including *Aggregatibacter actinomycetemcomitans* (*Aa*). Here we demonstrate the effectiveness of a silver lactate (SL)-containing RGD-coupled alginate hydrogel scaffold as a promising stem cell delivery vehicle with antimicrobial properties.

Materials and Methods—Gingival mesenchymal stem cells (GMSCs) or human bone marrow mesenchymal stem cells (hBMMSCs) were encapsulated in SL-loaded alginate hydrogel microspheres. Stem cell viability, proliferation, and osteo-differentiation capacity were analyzed.

Results—Our results showed that SL exhibited antimicrobial properties against *Aa* in a dose-dependent manner, with 0.50 mg/ml showing the greatest antimicrobial properties while still maintaining cell viability. At this concentration, SL-containing alginate hydrogel was able to inhibit *Aa* on the surface of Ti discs and significantly reduce the bacterial load in *Aa* suspensions. Silver ions were effectively released from the SL-loaded alginate microspheres for up to 2 weeks. Osteogenic differentiation of GMSCs and hBMMSCs encapsulated in the SL-loaded alginate

Correspondence. Alireza Moshaverinia, DDS, MS, PhD, FACP, Center for Craniofacial Molecular Biology (CCMB), Ostrow School of Dentistry, University of Southern California, 2250 Alcazar St. – CSA 103, Los Angeles, CA 90033. moshaver@usc.edu.

The authors declare no potential conflicts of interest with respect to the authorship and/or publication of this article.

microspheres were confirmed by the intense mineral matrix deposition and high expression of osteogenesis-related genes.

Conclusion—Taken together, our findings confirm that GMSCs encapsulated in RGD-modified alginate hydrogel containing SL show promise for bone tissue engineering with antimicrobial properties against *Aa* bacteria in vitro.

Keywords

Alginate hydrogel; antimicrobial properties; silver; mesenchymal stem cell; bone regeneration

Peri-implantitis is characterized by an inflammatory reaction in the tissues surrounding dental implants, with clinical features such as soft tissue inflammation (bleeding upon probing and suppuration) and progressive loss of supporting bone beyond biological bone remodeling.[1,2] Peri-implant bone loss is one of the most common inflammatory complications in craniofacial implantology.[1] Like periodontitis, peri-implantitis occurs mainly as a result of an overwhelming bacterial insult and subsequent host immune response.[1–3] It has been shown that bacterial species associated with periodontitis and periimplantitis are similar, including mainly Gram-negative anaerobes such as *Porphyromonas gingivalis*, *Prevotella intermedia*, and *Aggregatibacter actinomycetemcomitans* (*Aa*).[1–3] In particular, *Aa*, a facultative Gram-negative bacterium, appears to play an important role in certain types of periodontal disease.[4] *Aa*, or organisms likely to be *Aa*, have been isolated in high numbers from young patients with rapidly progressing alveolar bone breakdown.[4] It has been shown that *Aa* can form a biofilm on titanium implants, which can in turn be used as a colonizing surface, allowing in vivo bacterial persistence and inflammatory host response.[11] In addition, inflammatory cells, with B-lymphocytes and plasma cells being the most dominant among them, infiltrate the connective tissue adjacent to the pocket epithelium. Pro-inflammatory cytokines (e.g., IL-1, IL-6, IL-8, and TNF-α) are up-regulated in peri-implantitis.[6–8] Studies have confirmed that biofilm formation plays an important role in the initiation and progression of peri-implant disease and is critical for the development of infection around dental implants. Biofilm organisms differ significantly from their planktonic counterparts, as they are characterized by cells that have developed into a community rather than simply being attached to a surface.[9] These organisms are embedded in an extracellular polymer produced by bacterial cells. Furthermore, biofilm organisms exhibit an altered phenotype with respect to growth rate, gene transcription, and antimicrobial resistance.[10–12] Therefore, to introduce a predictable treatment modality for peri-implant bone loss, it is necessary to focus on managing the biofilm and biofilm organisms. Studies have shown that nonsurgical therapies might not be as effective as surgical treatment modalities.

Mesenchymal stem cells (MSCs) present an advantageous therapeutic option for bone tissue engineering in applications like this one. Recent studies have confirmed that MSCs derived from craniofacial structures such as gingival mesenchymal stem cells (GMSCs) have comparable differentiation capacities to bone marrow mesenchymal stem cells (BMMSCs).[13] Additionally, GMSCs are of particular interest as they can be harvested easily, are accessible through the oral cavity and can be obtained as discarded biological samples in dental clinics. Furthermore, MSCs possess profound immunomodulatory

properties and can inhibit the proliferation and function of several major types of immune cells (e.g., dendritic cells, T and B lymphocytes, and natural killer [NK] cells).[14,15] In addition, MSCs are known to have very low immunogenic properties due to low MHC class I expression levels and being negative for MHC class II.[16,17] It has been reported that MSC-mediated bone regeneration is partially controlled by the host local microenvironment, including the presence of growth factors as well as host immune cells and cytokines.[18] Scaffolds seeded with appropriate MSCs can create a suitable microenvironment for bone regeneration therapies, providing nutrients essential for prolonged cell viability, along with factors that promote osteogenic potential.[19–22] In our previous studies, we have shown that alginate hydrogel is a promising scaffold for the encapsulation of dental MSCs.[23,24] Alginates are natural heteropolysaccharides isolated from brown sea algae[25,26] with a wide variety of biomedical applications, including the encapsulation of cells and sensitive bioactive molecules, and are both injectable and biodegradable.[27,28] Recently, we have developed a novel 3D scaffold based on RGD-coupled alginate hydrogel for the encapsulation of GMSCs for bone regeneration.[23,24,29] However, alginate scaffolds containing antibacterial agents have never been used as a delivery vehicle for MSC-mediated bone regeneration as a treatment for biofilm-mediated peri-implant bone loss.

Silver (Ag) is one of the most widely used bactericidal agents available.[30] Ag is considered to have a broad antimicrobial spectrum and is less prone to microbial resistance than antibiotics, especially if rapid bactericidal action is achieved.[31,32] Although silver is relatively inert, its interaction with moisture leads to the release of silver ions, which are highly cytotoxic to microorganisms.[16] To achieve its biocidal effect, the required Ag dose is typically low enough to spare mammalian cell functions.[33] Many research groups have already explored the association of silver and biomaterials or have attached Ag to the implant itself as a means of preventing bacterial colonization, especially in the initial period after implant placement.[34–39]

A literature search failed to reveal any reports evaluating the application of GMSCs encapsulated in RGD-coupled alginate microspheres containing antimicrobial agents in bone regenerative therapy for peri-implantitis. Therefore, in the current study, we developed an injectable and 3D RGD-coupled alginate hydrogel cell encapsulation system containing silver lactate (SL). Considering the fact that GMSCs can be obtained as discarded biological samples from dental clinics and are easily harvested from the oral cavity, they can be considered ideal for stem cell banking purposes provided they show promise in MSC-based tissue regeneration. This approach was designed to optimize antimicrobial activity against a common periodontal pathogen (*Aa*) and to promote bone formation.

Materials and methods

Progenitor cell isolation and culture

Human GMSCs were isolated and cultured according to previously published procedures.[40] Teeth and gingival tissue were obtained from 20 healthy patients (18–25 years old) undergoing third molar extractions with IRB approval from the University of Southern California. Subjects with history of periodontal disease were excluded from this study. Human BMMSCs were processed from marrow aspirates of normal human adult volunteers

(20–35 years of age). MSCs were cultured in α-MEM (Invitrogen, Grand Island, NY) supplemented with 15% fetal bovine serum (FBS, Invitrogen), 180mMascorbic acid (Sigma-Aldrich, St. Louis, MO), 100 units/ml penicillin (Invitrogen), and 100 μg/ml streptomycin (Invitrogen). Passage four cells were used in all experiments.

Biomaterial fabrication, SL incorporation, and cell encapsulation

Custom-made RGD-coupled alginate with high guluronic acid content (NovaMatrix FMC Biopolymer, Sandvika, Norway) was used in this study. A 1% (w/v) sodium alginate solution was made with deionized water and sodium alginate according to our previous publications.[40–42] A stock solution of 5 mg/ml SL (Sigma-Aldrich) and alginate was prepared by agitation in a mixer overnight at room temperature. Five other concentrations (0.1, 0.25, 0.5, and 0.75 mg/ml SL) were prepared by serial dilution of the stock solution. The mixtures were agitated overnight at room temperature. Next, SL-loaded alginate microspheres were created by adding the solution dropwise to a 100 mM calcium chloride ($CaCl_2$) solution at 37°C. The microspheres were left to crosslink in the $CaCl_2$ solution for 7 minutes and subsequently rinsed with 0.9% NaCl solution.

GMSCs and hBMMSCs (as a positive control) were encapsulated separately in alginate loaded with SL. Cells were encapsulated at a density of 1×10^6 cells/ml of alginate solution. Microsphere formation was accomplished by adding the MSC-alginate mixture dropwise to 100 mM $CaCl_2$ solution. The resulting microspheres were incubated at 37°C for 45 minutes to complete cross-linking and then washed three times in nonsupplemented DMEM.

Cytotoxicity

The cytotoxicity of each SL-loaded alginate formulation was evaluated using a 3-(4,5-dimethylthiazol-2-yl)-2, 5-diphenyltetrazolium bromide (MTT) (Invitrogen) assay. GMSCs and hBMMSCs were plated at a cell density of 5×10^4 cells/ml in 96-well plates. After 24 hours, one microsphere of each SL-loaded alginate formulation was added to each well. Four replicate plates were made in total. After 24 hours and 7 days of culturing in regular media, microspheres were removed, and then 10 μl of the MTT solution was added to the cell monolayers. Next, 90 μl of α-MEM without supplementation was added to the wells. Plates were then incubated for 4 hours at 37°C in the dark. Formazan crystals formed during this process were extracted by adding 50 μl of dimethyl sulfoxide (DMSO). After 15 minutes, the absorbance was measured at 570 nm using a microplate reader.

SL activity against aggregatibacter actinomycetemcomitans (Aa)

Titanium disc surface treatment—The surfaces of machined $1.0 \times 1.0 \times 0.1$ cm^3 titanium (Ti) slabs were modified by grit blasting with silicon carbide (180 and 600) to produce rough surfaces before *Aa* inoculation.

Bacteria culture conditions—A purchased *A. actinomycetemcomitans* strain (ATCC® 33384™, Manassas, VA) was recovered from a lyophilized pellet and grown overnight in 5 ml of brain heart infusion broth (BHI; BD Biosciences, San Jose, CA) in an incubator (37°C, 5% CO_2, 220 rpm). The antimicrobial activity of the alginate microspheres containing

different concentrations of SL against the *Aa* was determined by qualitative (Parallel Streak Method) and quantitative evaluation (AATCC100).

Qualitative analysis of the inhibition zone—Microspheres containing 0, 0.5, and 2.5 mg/ml SL were placed on a lawn of bacteria on Ti discs on a BHI agar plate and incubated overnight at 37°C. Each lawn was prepared by spreading a 0.5 McFarland (optical density at 600 nm [OD600] of approximately 0.08–0.1) suspension of bacteria in broth using a sterile swab. Bactericidal activity was visually assessed to determine the zone of inhibition around each microsphere 24 hours and 5 days after contact of the microspheres with the inoculated bacterium. At least four replicates were performed for each experimental group. Four samples were randomly selected from each group, and then the diameter of the zone of inhibition, subtracted from the microsphere diameter, was calculated for each group and shown as distance in pixels using NIH Image J software (Version 1.64, NIH, Bethesda, MD).

Quantitative antimicrobial analysis of SL containing alginate microspheres—A direct quantitative evaluation of the antimicrobial activity of the SL incorporated in the alginate microspheres was also performed. Microspheres containing 0, 0.5, and 2.5 mg/ml SL (n = 10 microspheres per group) were soaked in 2 ml BHI broth inoculated with *Aa* at an initial concentration OD600 of 0.3. To control the accuracy of bacterial density, bacteria were serially diluted in PBS to 10^3, 10^4, 10^5, and 10^6 colony forming units (CFU/ml) and plated overnight (200 μl/plate). Suspensions were then incubated at 37°C for 24, 72, and 120 hours.

Release profile of SL—Sodium alginate microspheres containing two different concentrations of SL (n = 10 microspheres per group), 0.5 mg/ml (as best working concentration for eukaryotic cells), and 2.5 mg/ml, measuring approximately 20 μl each, were soaked in 1 ml double distilled water (ddH_2O) and maintained in an incubator at 37°C and 5% CO_2 for 24 hours and 7 and 14 days. Neutron activation analysis (NAA) (Elemental Analysis, Inc., Lexington, KY) was used to measure and quantify the concentration of silver ions released in ddH2O at each time point. NAA is a technique based on nuclear reactions whereby the element of interest is determined by irradiating the sample with neutrons, creating radioactive forms of the desired element, in this case Ag, in the sample. Counting is done using the relative amounts of detected gamma rays, which are proportional to the concentrations of the elements in the sample.[43]

In vitro osteogenic induction assay—Encapsulated GMSCs or hBMMSCs in alginate hydrogels (with or without SL) were cultured in osteogenic media containing 2 mM b-glycerophosphate (Sigma-Aldrich), 100 mM l-ascorbic acid 2-phosphate, and 10 nM dexamethasone (Sigma-Aldrich). Alginate microspheres without cells were used as a negative control (−). After 4 weeks of osteogenic induction, the osteogenic differentiation potential of encapsulated MSCs were analyzed using Alizarin red S (ARS) dye, which distinguishes the presence of calcified deposits. Briefly, the alginate hydrogel microspheres were fixed in 4% (v/v) paraformaldehyde for 30minutes prior to the serial dehydration process according to the methods already in the literature.[41,42] Next, 6-μm-thick paraffin

embedded sections were prepared. They were then stained with 2% (w/v) ARS dye solution for 5 minutes, and excess dye was removed by washing twice with deionizedwater. Images were captured using an Olympus DP50 digital camera (Olympus Optical Co., Miami, FL), and retained ARS was analyzed and quantified using NIH ImageJ software by determining the area positive for dye staining expressed as a fraction of the total area.

RNA isolation, reverse transcription and real-time PCR—GMSCs and hBMMSCs were encapsulated in SL-loaded alginate hydrogels, and after 2 weeks of osteogenic differentiation, 10 alginate hydrogel microcapsules were collected and dissolved in an sterile depolymerization buffer consisting of 50 mM sodium citrate dehydrate and 80 mM sodium chloride (Sigma Aldrich) for 20 minutes. Following dissolution, the de-capsulated cells were centrifuged at 10,000 × *g* for 10 minutes, and the pellet was washed with PBS and centrifuged again at 10,000 × *g* for 3 minutes. Total RNA was extracted using Trizol reagent (Invitrogen) according to the manufacturer's recommendations. Single-stranded cDNA synthesis was performed with 100 ng total RNA using a Superscript III cDNA synthesis kit (Invitrogen). Data were analyzed using the $2^{-\Delta\Delta Ct}$ method, with normalization to the Ct of the housekeeping gene GAPDH. Primer and probe sequences are described in Table 1.

SEM analysis

To characterize the morphology of the alginate scaffolds and encapsulated cells, scanning electron microscopy (SEM) (JEOL 5300, Peabody, MA) was used. In addition, the lawn of bacteria on the Ti disc surfaces after 5 days in contact with the alginate microspheres containing 0.5 mg/ml SL was also visualized by SEM. Briefly, samples were fixed with glutaraldehyde 2.5% in PBS, washed twice in 0.1 M cacodylate buffer, and post-fixed with 2% osmium tetroxide in 0.1 M cacodylate buffer. Then, samples were dehydrated in graded alcohol (50%, 70%, 85%, 95%, and 100%) and alcohol/HDMS (v/v) (50/50, 75/25, 85/15, and 95/5). Next, samples were left to dry overnight, mounted in metal stubs and sputter coated with gold (25 mA, 10^{-1} vacuum, 2 minutes).

Statistical analysis

Quantitative data were expressed as mean and standard deviation (SD). One-way and two-way ANOVA, followed by Tukey test at a significance level of a=0.05, were used for comparison among multiple sample means.

Results

In this in vitro study, we developed a 3D MSC delivery vehicle based on alginate and tuned for the local delivery of SL with a defined and predictable drug release profile (Fig 1). After 24 hours or 7 days, cell monolayers in contact with the SL-loaded alginate microspheres were evaluated using MTT assays. Both GMSCs and hBMMSCs exhibited dose-dependent cytotoxicity when in contact with SL at a concentration of 0.1 to 0.75 mg/ml (Fig 2). Regardless of the cell type and time interval assessed, cell viability started to decrease when SL was used at concentrations above 0.5 mg/ml. After 24 hours, SL-loaded alginate at 0.75 mg/ml significantly reduced cell viability in comparison to all other concentrations, irrespective of the cell type ($p < 0.05$) (Fig 2A). After 7 days in culture, SL-loaded alginate

at 0.75 mg/ml had significantly lower cell viability than the control group, for GMSC and hBMMSC cultures ($p < 0.05$) (Fig 2B).

The release profiles of silver ions from the alginate incorporated with two SL concentrations were evaluated after 24 hours and 7 and 14 days by NAA. The results showed sustained release of silver ions for up to 14 days (Fig 3).

According to the obtained SL cytotoxicity data, 0.5 mg/ml was selected as the optimal concentration for the investigation of antimicrobial activity of the SL-loaded alginate against *Aa* bacteria. An SL concentration 5× greater (2.5 mg/ml) was used for comparison. Alginate alone was used as a negative control. After 1 and 5 days, qualitative analysis of the antimicrobial properties of the SL-loaded alginate against a biofilm layer of *Aa* seeded on the surface ofTi discs indicated zones of inhibition (ZI) around all scaffolds with SL incorporation (Parallel Streak Method) (Fig 4). No ZI was observed against bacteria in the group in which alginate was used without the SL (Fig 4A).SEM analysis of the Ti discs with *Aa* biofilm in contact with a 0.5 mg/ml SL-loaded alginate microsphere confirmed the presence of a ZI produced by the antimicrobial agent (Fig 5).

Quantitatively, there was no significant difference in the ZI size in the 0.5 mg/ml and 2.5 mg/ml SL groups after 24 hours of contact with the *Aa* (Fig 6A). After 5 days, the ZI of both SL concentrations were significantly smaller than at 24 hours ($p < 0.05$). Moreover, the ZI of the 0.5 mg/ml group after 5 days was larger than that of the 2.5 mg/ml group ($p = 0.035$); meanwhile, there was significant microsphere shrinkage in the 2.5 mg/ml group ($p = 0.044$).

The antimicrobial activity of SL was also tested in *Aa* suspensions (Fig 6B). After 24 and 72 hours, all SL-loaded alginate concentrations were able to significantly ($P < 0.05$) reduce the *Aa* bacterial load. After 120 hours (5 days), the antimicrobial activity against *Aa* suspensions was no longer observed for SL-loaded alginate with concentrations less than 0.5 mg/ml.

Next, GMSCs and hBMMSCs were encapsulated in the 0.5-mg/ml SL-loaded alginate and osteo-differentiation of encapsulated MSCs was analyzed in the presence of the antimicrobial agent. The expression levels of the osteogenic genes *RUNX2* and *PCN* were confirmed and compared via RT-PCR. Our results revealed that GMSCs as well as hBMMSCs expressed *RUNX2* and *OCN* abundantly after 2 weeks under osteogenic induction in the presence of in 0.5 mg/ml SL (Fig 7). The osteogenic differentiation of encapsulated GMSCs or hBMMSCs in SL-containing alginate hydrogels were analyzed using Alizarin red S (ARS) staining. After 4 weeks, both GMSC and hBMMSC groups differentiated into nodules that stained positively with ARS, indicative of their osteogenic fate (Fig 8A), while the negative control group (alginate alone with no induction) failed to exhibit any positive staining. The quantification of the mineral matrix deposition using Image J confirmed that both GMSCs and hBMMSCs produced significantly more mineral nodules than the negative control (Fig 8B). The results confirmed the possibility of osteo-differentiation of encapsulated GMSCs in the presence of SL at an optimized concentration.

Discussion

Peri-implant bone loss remains a serious surgical complication that is difficult to treat. Accordingly, the avoidance of biofilm buildup on implants is well recognized as being necessary to guarantee the success of dental implants, preventing their loss and the need for secondary surgeries; however, besides combating the bacterial buildup, for a successful surgical outcome it is also necessary to promote tissue integration and repair. Here we incorporated SL in sodium alginate scaffolds to prevent bacterial contamination and accelerate bone formation, especially in the initial period after implant placement. We observed that SL-loaded alginate at 0.5 mg/ml was effective in preventing *A. actinomycetemcomitans* (*Aa*) growth in biofilms and in suspensions. Furthermore, GMSCs and hBMMSCs encapsulated in the biomaterial showed excellent osteoconductivity, once MSCs were able to differentiate into osteoblast-like cells and deposit a remarkable amount of mineral matrix.

We first investigated the cytotoxicity of a range of SL concentrations incorporated in alginate microspheres and assessed their effects on the viability of GMSCs and hBMMSCs cell cultures to select a biocompatible SL concentration. SL had a dose-dependent effect on the viability of both types of MSCs. Regardless of the cell type and time interval assessed, cell viability started to decrease when SL was used at concentrations at or above 0.5 mg/ml. SL at 0.5 mg/ml was slightly cytotoxic and was selected to further investigate the SL antimicrobial activity on *Aa* bacteria. Our results are in line with other findings in which biomaterials containing proper concentrations of Ag were shown to be compatible with eukaryotic cells, such as fibroblasts and osteoblasts.[44–47]

We used a commercial *Aa* strain to further confirm the bacterial activity of SL-containing alginate hydrogels. When in contact with a lawn of *Aa* bacteria seeded on Ti discs, alginate loaded with SL at a concentration of 0.5 mg/ml or 2.5 mg/ml presented clear zones of inhibition (ZI) around all scaffolds. SEM analysis depicted morphological changes in bacteria cells immediately in contact with the biomaterial and a large accumulation of bacteria in the ZI. After 24 and 72 hours of contact, planktonic cultures of *Aa* were sensitive to both SL-loaded alginate concentrations, significantly reducing the bacterial load in the suspensions. At 120 hours, the antimicrobial efficacy diminished. It should be noted that the bacterial load ($>10^8$ CFU/ml) tested here was much larger than what is commonly observed in contaminated implants in vivo (around 10^3 CFU/ml).[48] Moreover, the antimicrobial activity of SL-loaded alginate was tested in 2 ml of broth, instead of PBS—a situation where bacterial growth was being stimulated. Considering its performance in these highly adverse conditions, SL-loaded alginate may be able to inhibit bacterial growth for longer periods in vivo.

Paul et al[49] tested the antimicrobial activity of silver-particle-incorporated polyurethane films (1% or 10% [w/w] $AgNO_3$ and 1% or 10% [w/w] SL) against *Escherichia coli* and *Staphylococcus aureus*. They reported that SL performed better than silver nitrate in inhibiting bacterial growth, even at a low concentration of 1% (w/w) SL. This concentration is close to the one investigated in our study (0.5 mg/ml or 5% [w/w]). *S. aureus* (Gram positive) was less sensitive to the silver antimicrobials than *E. coli* (Gram negative). Other

reports corroborate these findings, reporting that the lipopolysaccharide walls of Gram-negative bacteria likely provide an electrostatically attractive surface for silver ions.[49] Silver has antimicrobial activity against a broad range of periodontal pathogens, which are predominantly Gram-negative, such as the *Aa* tested here.

As has been previously reported, the antimicrobial activity of silver is dependent on the silver cations, which bind strongly to electron donor groups in biological molecules containing sulfur, oxygen, or nitrogen.[39] The highly reactive ionized silver binds to tissue proteins and produces structural changes in the bacterial cell wall and nuclear membrane, leading to cell distortion and death.[15] Moreover, the binding of silver to bacterial DNA and RNA inhibits bacterial replication.[51,52] The use of silver has been investigated as a potential risk to human health and environmental biota depending on the grade of silver used. Following their entry into systemic circulation, silver particles can migrate and induce toxicity to many organs.[53] On a cellular level, silver is internalized by macrophages and sorted to the cytoplasm. Intracellularly, released silver ions interfere with mitochondrial functions and induce apoptotic cell death. Nevertheless, eukaryotic cells show higher structural and functional redundancy than prokaryotic cells. Thus, much higher silver ion concentrations (more than 1.6 ppm Ag ions)[54] are required to achieve comparable toxic effects in eukaryotic cells than in prokaryotic ones.

Our silver release profile study has shown that in the first 24 hours, silver ion levels were at or below 0.04 ppm. The release of silver ions from both studied starting concentrations could be detected for up to 7 days (0.05 and 0.06 ppm, respectively). After 14 days, silver ions were undetectable due to being below the precision limit of the NAA equipment (0.04 ppm) for the 0.5 mg/ml starting concentration of SL. Nevertheless, the biocidal effect of silver seems to be active at a concentration as low as 0.1 ppb.[55] Accordingly, despite our limitation in quantifying low levels of silver, it is likely that the alginate is able to provide a sustained release of Ag, as it gradually degrades for several months.[51]

Besides the antimicrobial activity of SL-loaded alginate, we also investigated its osteoconductivity by encapsulating MSCs in the biomaterial. A large amount of mineralized nodule formation was observed in both the GMSC and hBMMSC groups. After 2 weeks of encapsulation, both cells were expressing genes related to osteodifferentiation, namely *RUNX2* and *OCN*. To the best of our knowledge, this is the first time that alginate hydrogel containing SL has been used for encapsulation of GMSCs and investigated as a treatment modality for peri-implantitis. A recent study has shown that silver particles do not impair bone formation by the osteosarcoma MG-63 human cell line.[56] Sun et al[57] have reported successful results associating silver nanoparticles, collagen, and bone morphogenetic protein 2 for the regeneration of bone in infected wounds. One especially promising property of our biomaterial is that, even in the presence of an antimicrobial agent, bone formation was extensively achieved using GMSCs and hBMMSCs without any additional component, such as a growth factor.

Conclusion

A novel noninvasive treatment modality for management of peri-implantitis and peri-implant bone loss was introduced based on a micro-encapsulation system that delivers GMSCs encapsulated in a scaffold of RGD-coupled alginate. This injectable and biodegradable scaffold can be imbued with antimicrobial properties through the addition of SL. It was shown that encapsulated GMSCs in SL-containing alginate hydrogel successfully differentiated into osteogenic tissue. The proposed system possesses the synergistic bone regenerative properties of GMSCs and the antibacterial properties of SL and can be used as a novel treatment modality for biofilm-mediated periimplant bone loss.

Acknowledgments

This work was supported by grants from the GSK Prosthodontist Innovator Award from the American College of Prosthodontists Education Foundation (ACPEF) to A.M. and the National Institute for Dental and Craniofacial Research (K08DE023825 to A.M. and R01 DE017449 to S.S.).

References

1. Lindhe J, Meyle J. Peri-implant diseases: consensus report of the Sixth European Workshop on Periodontology. J Clin Periodontol. 2008; 35:282–285. [PubMed: 18724855]
2. Sanz M, Chapple IL. Clinical research on peri-implant diseases: consensus report of Working Group 4. J Clin Periodontol. 2012; 39:202–206. [PubMed: 22533957]
3. Koldsland OC, Scheie A, Aass AM. Prevalence of peri-implantitis related to severity of the disease with different degrees of bone loss. J Periodontol. 2010; 81:231–238. [PubMed: 20151801]
4. Slots J, Reynolds HS, Genco RJ. Actinobacillus actinomycetemcomitans in human periodontal disease: a cross-sectional microbiological investigation. Infect Immun. 1980; 29:1013–1020. [PubMed: 6968718]
5. Rinke S, Ohl S, Ziebolz D, et al. Prevalence of peri-implant disease in partially edentu- lous patients: a practice-based cross-sectional study. Clin Oral Implants Res. 2011; 22:826–833. [PubMed: 21198898]
6. Mombelli A, Long NP. The diagnosis and treatment of peri-implantitis. Periodontal 2000. 1998; 17:63–76.
7. Fransson C, Lekholm U, Jemt T, et al. Prevalence of subjects with progressive bone loss at im plants. Clin Oral Implants Res. 2005; 16:440–446. [PubMed: 16117768]
8. Roos-Jansåker AM, Lindahl C, Renvert H, et al. Nine- to fourteen-year follow-up of implant treatment. Part II: presence of peri-implant lesions. J Clin Periodontol. 2006; 33:290–295. [PubMed: 16553638]
9. Haffajee AD, Socransky SS. Introduction to microbial aspects of periodontal biofilm communities, development and treatment. Periodontol 2000. 2006; 42:7–12. [PubMed: 16930302]
10. Donlan RM, Costerton JW. Biofilms: survival mechanisms of clinically relevant microorganisms. Clin Microbiol Rev. 2002; 15:167–193. [PubMed: 11932229]
11. Freire MO, Sedghizadeh PP, Schaudinn C, et al. Development of an animal model for Aggregatibacter actinomycetemcomitans biofilm-mediated oral osteolytic infection: a preliminary study. J Periodontol. 2011; 82:778–789. [PubMed: 21222546]
12. Patel R. Biofilms and antimicrobial resistance. Clin Orthop Relat Res. 2005; 437:41–47. [PubMed: 16056024]
13. Zhang QZ, Nguyen AL, Yu WH, et al. Human oral mucosa and gingiva: a unique reservoir for mesenchymal stem cells. J Dent Res. 2012; 91:1011–1018. [PubMed: 22988012]
14. Nauta AJ, Fibbe WE. Immunomodulatory properties of mesenchymal stromal cells. Blood. 2007; 110:3499–3506. [PubMed: 17664353]

15. Pittenger MF, Mackay AM, Beck SC, et al. Multilineage potential of adult human mesenchymal stem cells. Science. 1999; 284:143–147. [PubMed: 10102814]
16. English K, French A, Wood KJ. Mesenchymal stromal cells: facilitators of successful transplantation? Cell Stem Cell. 2010; 7:431–442. [PubMed: 20887949]
17. Undale AH, Westendorf JJ, Yaszemski MJ, et al. Mesenchymal stem cells for bone repair and metabolic bone diseases. Mayo Clin Proc. 2009; 84:893–902. [PubMed: 19797778]
18. Liu Y, Wang L, Kikuiri T, et al. Mesenchymal stem cell-based tissue regeneration is governed by recipient T lymphocytes via IFN-gamma and TNF-alpha. Nat Med. 2011; 17:1594–1601. [PubMed: 22101767]
19. Anderson DG, Levenberg S, Langer R. Nanoliter-scale synthesis of arrayed biomaterials and application to human embryonic stem cells. Nat Biotechnol. 2004; 22:863–866. [PubMed: 15195101]
20. Engler AJ, Sen S, Sweeney HL, et al. Matrix elasticity directs stem cell lineage specification. Cell. 2006; 126:677–689. [PubMed: 16923388]
21. Valamehr B, Jonas SJ, Polleux J, et al. Hydrophobic surfaces for enhanced differentiation of embryonic stem cell-derived embryoid bodies. Proc Natl Acad Sci U S A. 2008; 105:14459–14464. [PubMed: 18791068]
22. Sapir Y, Kryukov O, Cohen S. Integration of multiple cell-matrix interactions into alginate scaffolds for promoting cardiac tissue regeneration. Biomaterials. 2011; 7:1838–1847. [PubMed: 21112626]
23. Moshaverinia A, Chen C, Akiyama K, et al. Alginate hydrogel as a promising scaffold for dental-derived stem cells: an in vitro study. J Mater Sci Mater Med. 2012; 23:3041–3051. [PubMed: 22945383]
24. Moshaverinia A, Chen C, Akiyama K, et al. Encapsulated dental-derived mesenchymal stem cells in an injectable and biodegradable scaffold for applications in bone tissue engineering. J Biomed Mater Res A. 2013; 101:3285–3294. [PubMed: 23983201]
25. Smidsrod O, Skjakbraek G. Alginate as immobilization matrix for cells. Trends Biotechnol. 1990; 8:71–78. [PubMed: 1366500]
26. Alsberg A, Anderson KW, Albeiruti A, et al. Cell-interactive alginate hydrogels for bone tissue engineering. J Dent Res. 2001; 80:2025–2029. [PubMed: 11759015]
27. Evangelista MB, Hsiong SX, Fernandes R, et al. Upregulation of bone cell differentiation through immobilization within a synthetic extracellular matrix. Biomaterials. 2007; 28:3644–3655. [PubMed: 17532040]
28. Gautier A, Carpentier B, Dufresne M, et al. Impact of alginate type and bead diameter on mass transfer and the metabolic activities of encapsulated C3A cells in bioartificial liver applications. Eur Cell Mater. 2011; 21:94–106. [PubMed: 21267945]
29. Moshaverinia A, Chen C, Xu X, et al. Bone regeneration potential of stem cells derived from periodontal ligament or gingival tissue sources encapsulated in RGD-modified alginate scaffold. Tissue Eng Part A. 2014; 20:611–621. [PubMed: 24070211]
30. Sharma VK, Yngard RA, Lin Y. Silver nanoparticles: green synthesis and their antimicrobial activities. Adv Colloid Interface Sci. 2009; 145:83–96. [PubMed: 18945421]
31. Chopra I. The increasing use of silver based products on antimicrobial agents: a useful development or a cause for concern? J Antimicrob Chemother. 2007; 59:587–590. [PubMed: 17307768]
32. Chiu T, Burd A. “Xenograft” dressing in the treatment of burns. Clin Dermatol. 2005; 23:419–423. [PubMed: 16023938]
33. Rai M, Yadav A, Gade A. Silver nanoparticles as a new generation of antimicrobials. Biotechnol Adv. 2009; 27:76–83. [PubMed: 18854209]
34. Alt V, Bechert T, Steinrucke P, et al. An in vitro assessment of the antibacterial properties and cytotoxicity of nanoparticulate silver bone cement. Biomaterials. 2004; 25:4383–4391. [PubMed: 15046929]
35. Bellantone M, Coleman NJ, Hench LL. Bacteriostatic action of a novel four-component bioactive glass. J Biomed Mater Res. 2000; 51:484–490. [PubMed: 10880092]

36. Kumar R, Münstedt H. Silver ion release from antimicrobial polyamide/silver composites. Biomaterials. 2005; 26:2081–2088. [PubMed: 15576182]
37. Ewald A, Glückermann SK, Thull R, et al. Antimicrobial titanium/silver PVD coatings on titanium. Biomed Eng Online. 2006; 5:22. [PubMed: 16556327]
38. Lim PN, Teo EY, Ho B, et al. Effect of silver content on the antibacterial and bioactive properties of silver-substituted hydroxyapatite. J Biomed Mater Res A. 2013; 101:2456–2464. [PubMed: 23349126]
39. Roohpour N, Moshaverinia A, Wasikiewicz JM, et al. Development of bacterially resistant polyurethane for coating medical devices. Biomed Mater. 2012; 7:015007. [PubMed: 22287552]
40. Zhang Q, Shi S, Liu Y, et al. Mesenchymal stem cells derived from human gingiva are capable of immunomodulatory functions and ameliorate inflammation-related tissue destruction in experimental colitis. J Immunol. 2009; 183:7787–7798. [PubMed: 19923445]
41. Ansari S, Moshaverinia A, Han A, et al. Functionalization of scaffolds with chimeric anti-BMP-2 monoclonal antibodies for osseous regeneration. Biomaterials. 2013; 34:10191–10198. [PubMed: 24055525]
42. Moshaverinia A, Ansari S, Chen C, et al. Co-encapsulation of anti-BMP2 monoclonal antibody and mesenchymal stem cells in alginate microspheres for bone tissue engineering. Biomaterials. 2013; 34:6572–6579. [PubMed: 23773817]
43. Yang H, Gao LN, An Y, et al. Comparison of mesenchymal stem cells derived from gingival tissue and periodontal ligament in different incubation conditions. Biomaterials. 2013; 34:7033–7047. [PubMed: 23768902]
44. Moshaverinia A, Xu X, Chen C, et al. Application of stem cells derived from the periodontal ligament or gingival tissue sources for tendon tissue regeneration. Biomaterials. 2014; 35:2642–2650. [PubMed: 24397989]
45. Zhao L, Chu PK, Zhang Y, et al. Antibacterial coatings on titanium implants. J Biomed Mater Res B Appl Biomater. 2009; 91:470–480. [PubMed: 19637369]
46. Bosetti M, Masse A, Tobin E, et al. Silver coated materials for externalixation devices: in vitro biocompatibility and genotoxicity. Biomaterials. 2002; 23:887–892. [PubMed: 11771707]
47. Mohiti-Asli M, Pourdeyhimi B, Loboa EG. Novel, silver-ion-releasing nanofibrous scaffolds exhibit excellent antibacterial efficacy without the use of silver nanoparticles. Acta Biomater. 2014; 10:2096–2104. [PubMed: 24365706]
48. Dörtbudak O, Haas R, Bernhart T, et al. Lethal photosensitization for decontamination of implant surfaces in the treatment of peri-implantitis. Clin Oral Implants Res. 2001; 12:104–108. [PubMed: 11251658]
49. Paul D, Paul S, Roohpour N, et al. Antimicrobial, mechanical and thermal studies of silver particle-loaded polyurethane. J Funct Biomater. 2013; 4:358–375. [PubMed: 24956194]
50. Shrivastava S, Bera T, Roy A, et al. Characterization of enhanced antibacterial effects of novel silver nanoparticles. Nanotechnology. 2007; 18:225103.
51. Lansdown AB. Silver: 1. Its antibacterial properties and mechanism of action. J Wound Care. 2002; 11:125–130. [PubMed: 11998592]
52. Lansdown AB. Silver: 2. Toxicity in mammals and how its products aid wound repair. J Wound Care. 2002; 11:173–177. [PubMed: 12055941]
53. Tang J, Xiong L, Wang S, et al. Distribution, translocation and accumulation of silver nanoparticles in rats. J Nanosci Nanotechnol. 2009; 9:4924–4932. [PubMed: 19928170]
54. Hidalgo E, Domínguez C. Study of cytotoxicity mechanisms of silver nitrate in human dermal fibroblasts. Toxic Lett. 1998; 98:169–179.
55. Ciobanu CS, Iconaru SL, Le Coustumer P, et al. Antibacterial activity of silver-doped hydroxyapatite nanoparticles against gram-positive and gram-negative bacteria. Nanoscale Res Lett. 2012; 7:324–333. [PubMed: 22721352]
56. Marsich E, Bellomo F, Turco G, et al. Nano-composite scaffolds for bone tissue engineering containing silver nanoparticles: preparation, characterization and biological properties. J Mater Sci Mater Med. 2013; 24:1799–1807. [PubMed: 23553569]

57. Sun CY, Che YJ, Lu SJ. Preparation and application of collagen scaffold-encapsulated silver nanoparticles and bone morphogenetic protein 2 for enhancing the repair of infected bone. Biotechnol Lett. 2015; 37:467–473. [PubMed: 25326174]

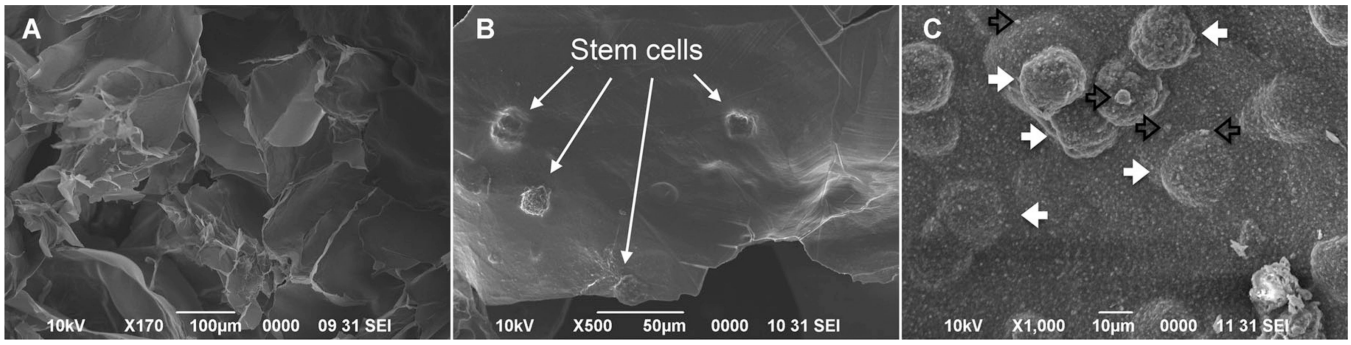

Figure 1.

SEM image of the alginate hydrogel alone (A) and alginate-MSC construct (B) showing encapsulated MSCs within porous (C) alginate hydrogel microspheres after 2 weeks of culturing in regular media. Silver particles (open black arrows) are observed in close contact with encapsulated MSCs (solid white arrows).

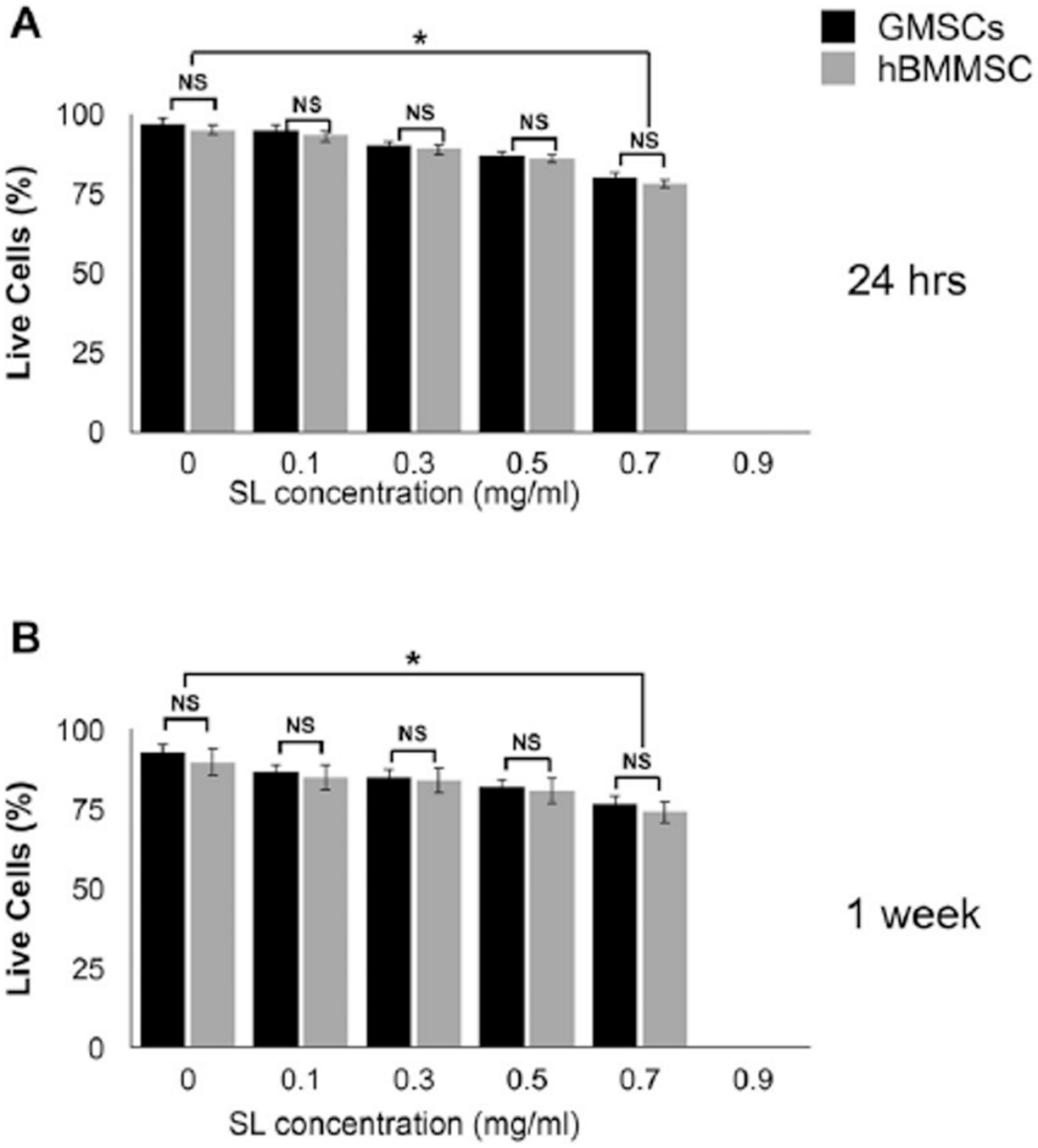

Figure 2.

Cytotoxicity of a range of concentrations of silver lactate (SL) incorporated into alginate microspheres after 24 hours (A) and 7 days (B) in contact with GMSCs and hBMMSCs.

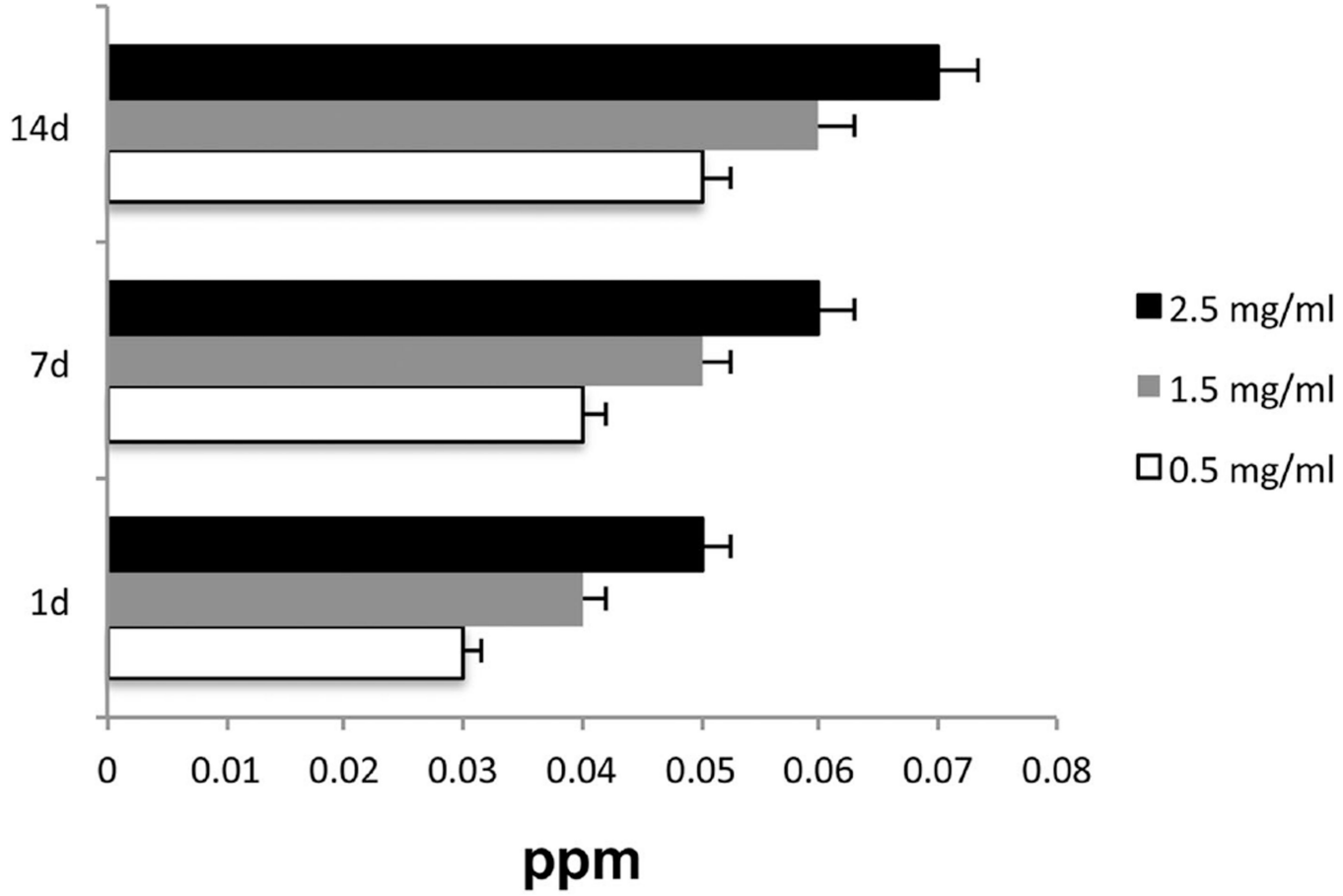

Figure 3.
Silver-releasing profile characteristics from alginate hydrogel.

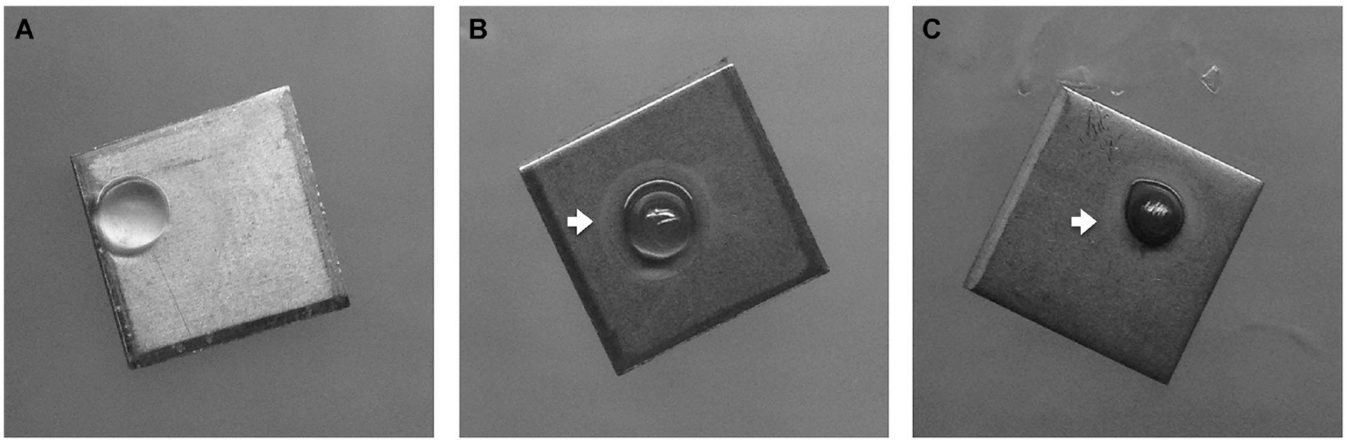

Figure 4.
Zone of inhibition produced by the 0 mg/ml (A), 0.5 mg/ml (B) and 2.5 mg/ml (C) SL-containing alginate microspheres (white arrows).

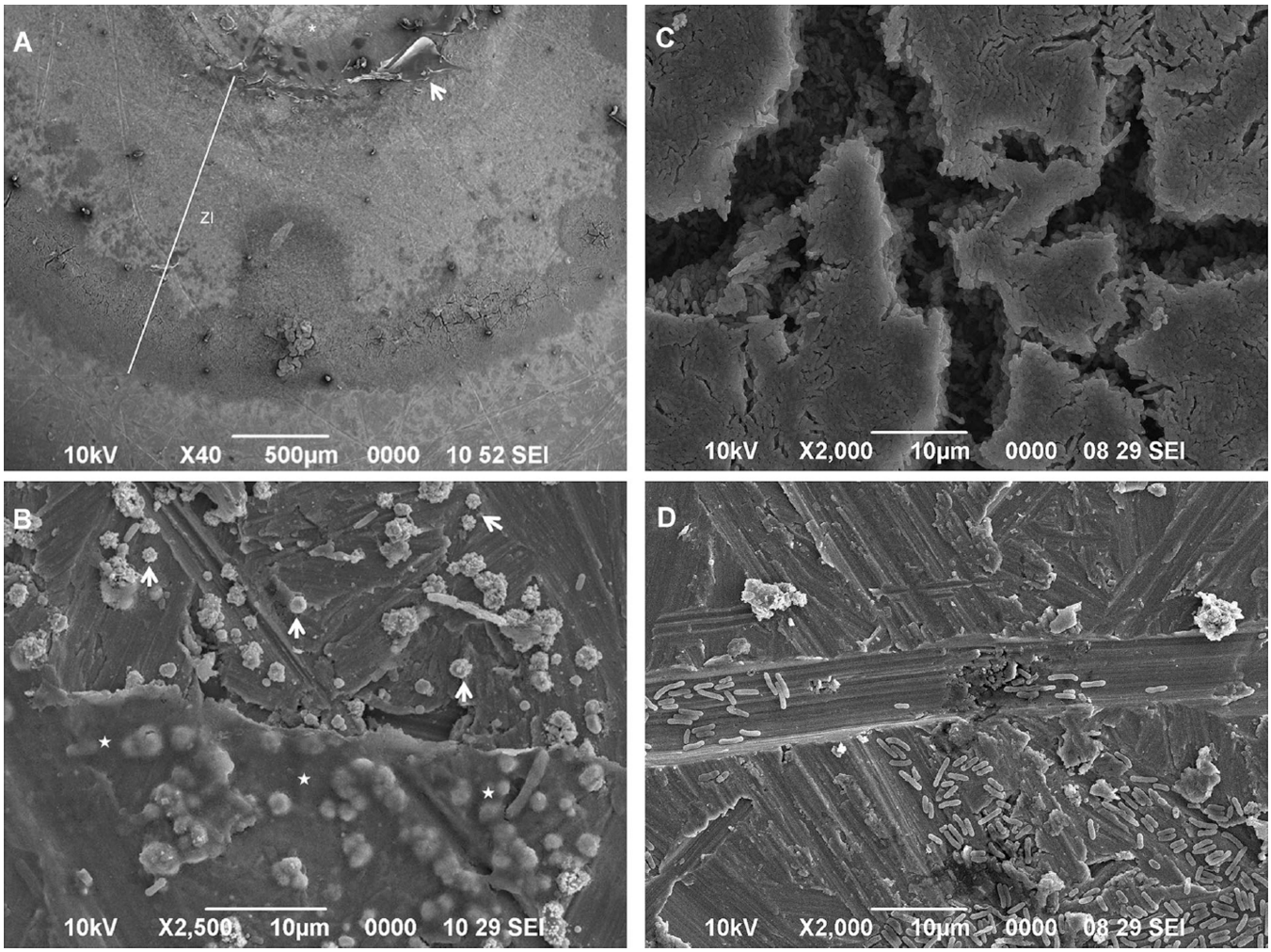

Figure 5.

SEM analysis depicting bacterial distribution and morphology along the Ti disc surface covered with *Aa* after contact with the 0.5 mg/ml SL alginate microsphere. (A) Interfaces produced by the contact of the 0.5 mg/ml SL alginate microspheres. Zone of inhibition, ZI; surface previously covered by the microsphere, *; residues of hydrogel, arrow. (B) Closer view of residue of the hydrogel. Round shaped *Aa* (arrows) suggest bacterial death near the biomaterial (⋆). (C) *Aa* aggregates in the outer part of the ZI. (D) *Aa* distribution on the Ti disc surface outside the ZI.

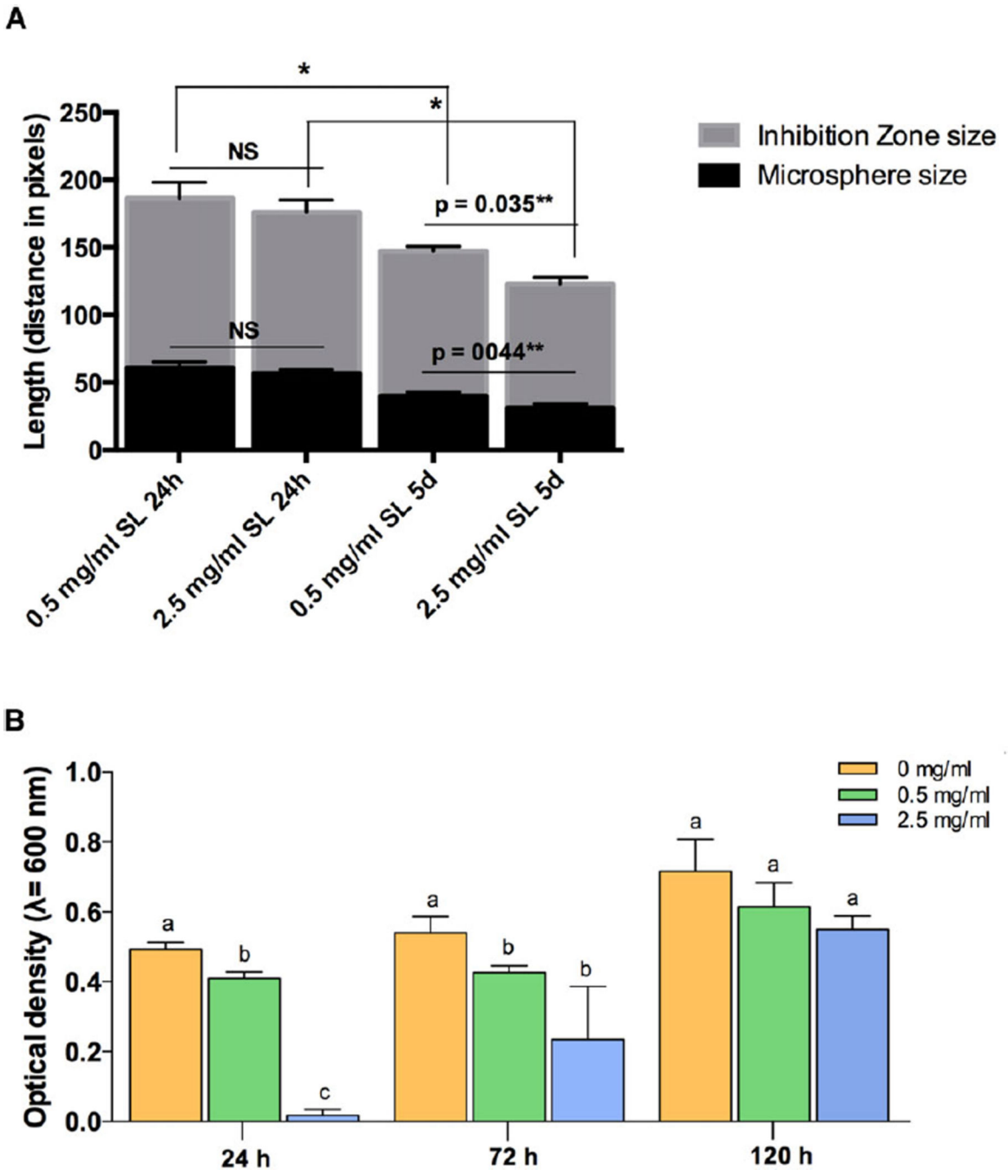

Figure 6.

(A) Zone of inhibition quantification in relation tomicrosphere shrinkage for both SL concentrations after 24 hours and 5 days. (B) Antimicrobial activity of 0.5 mg/ml and 2.5 mg/ml SL concentrations against *Aa* suspensions after 1, 3, and 5 days. Different letters show significant differences (*$p < 0.05$) between groups at the same time points. Asterisks show significant differences between groups. *$p < 0.05$, **$p < 0.01$.

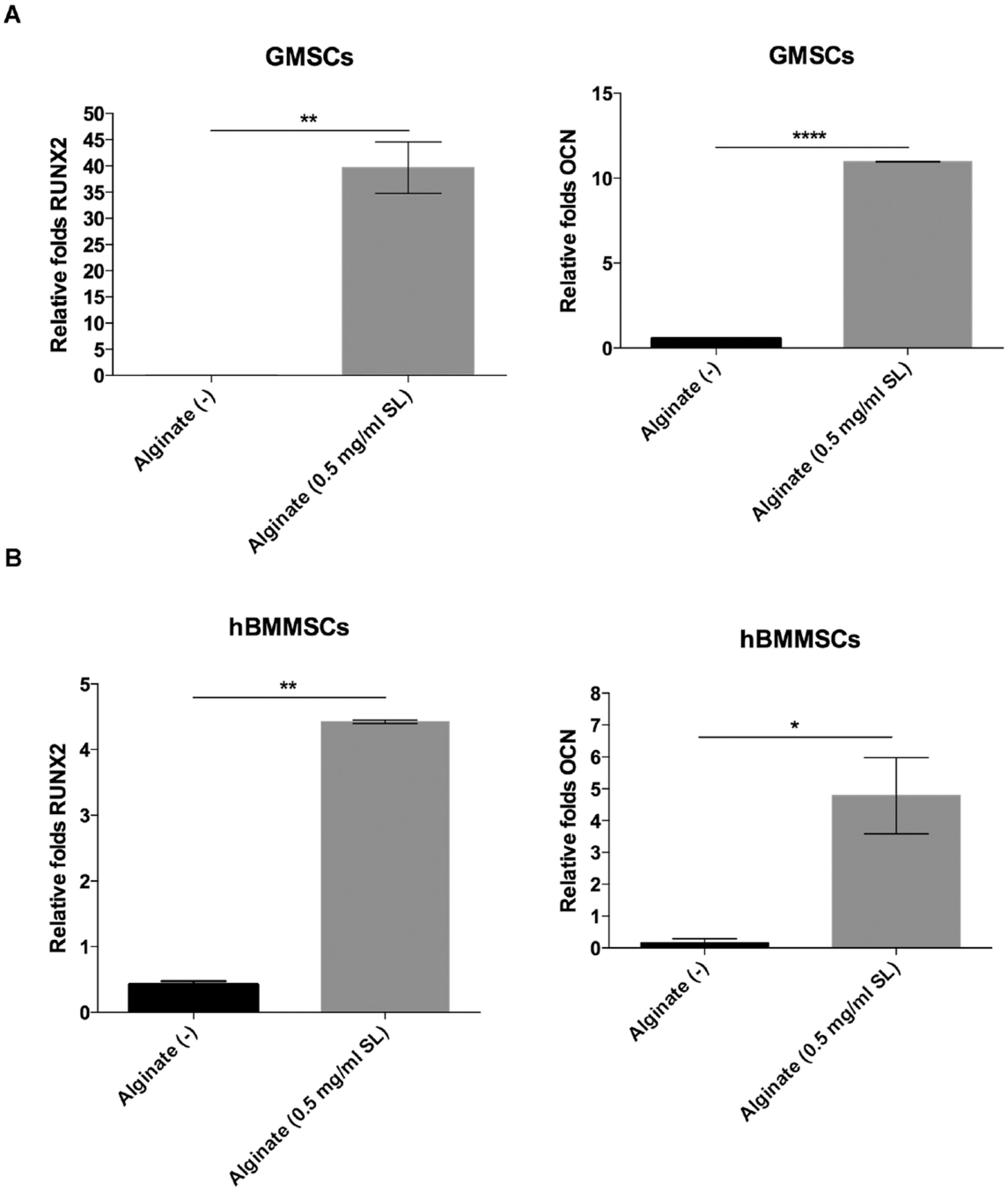

Figure 7.

Specific gene expression for osteogenic differentiation of encapsulated MSCs in vitro. Expression level (in fold changes) of OCN and RUNX2 genes for each encapsulated GMSC (A) and hBMMSC (B) after 2 weeks of culturing in induction media in vitro evaluated by RT-PCR. Data were normalized by the Ct of the housekeeping gene GAPDH and expressed relative to the expression level for the same gene at day 1.

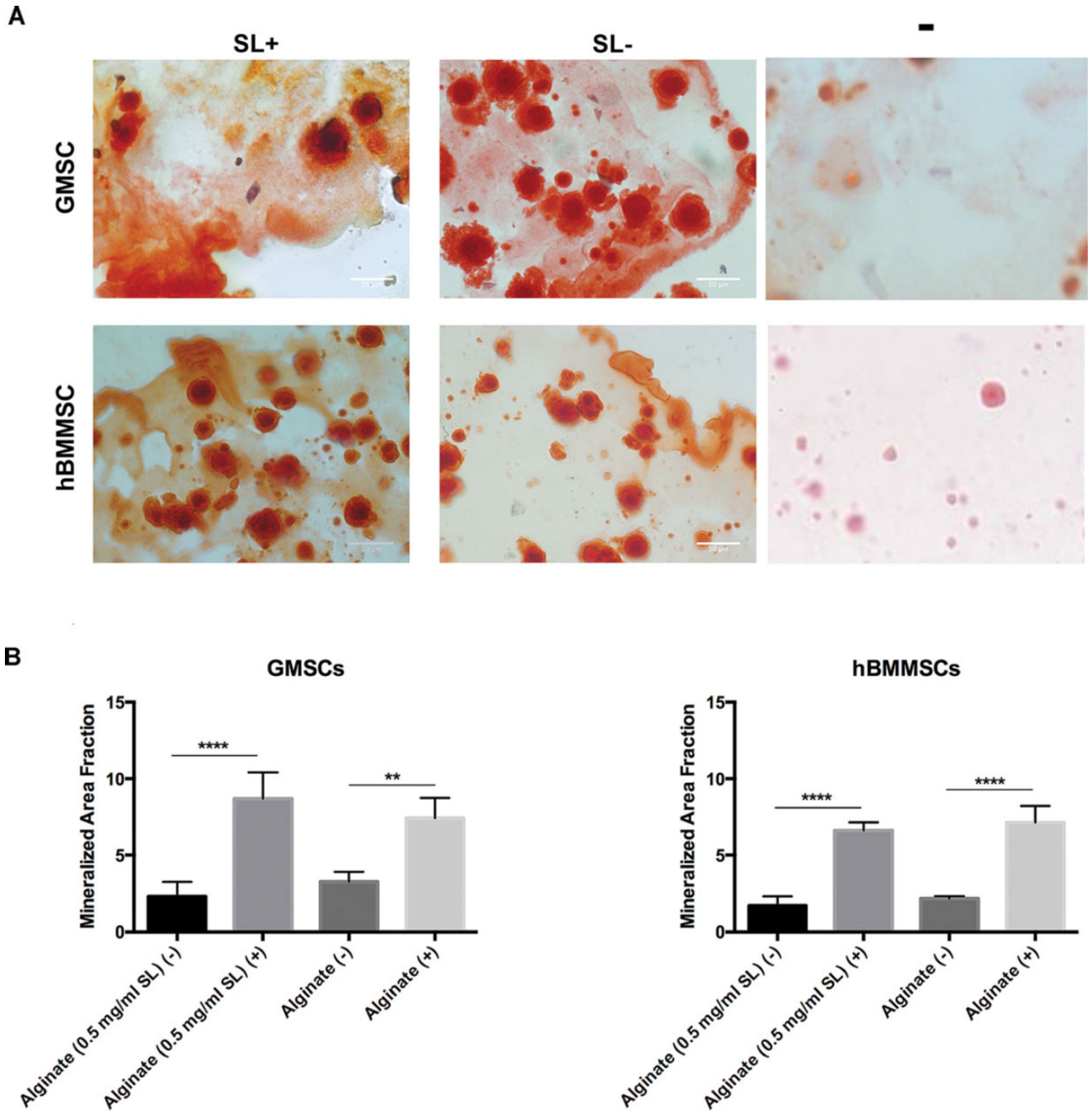

Figure 8.

Qualitative (A) and quantitative (B) measurement of calcium deposition localized to biomineralized MSC-alginate constructs using Alizarin red dye showing the osteo-differentiation capacity of GMSCs and hBMMSCs encapsulated in alginate with (SL +) and without SL (SL −). Control groups without mineralization induction were used as the negative control (−) while encapsulated MSCs without SL (SL −) were used as the positive group.

Table 1

Oligonucleotide primers used in PCR analysis

Gene	Sequence	Product (bp)
Runt-related transcription factor 2 (Runx2)	Sense: 5′-CAGTTCCCAAGCATTTCATCC-3′; Antisense: 5′-TCAATATGGTCGCCAAA CAG-3′	289
Osteocalcin (OCN)	Sense: 5′-CATGAGAGCCCTCACA-3′; Antisense: 5′-AGAGCGACACCCTAGAC-3′	292
Glyceraldehyde 3-phosphate dehydrogenase (GADPH)	Sense: 5′-AGCCGCATCTTCTTTTGCGTC-3′: Antisense: 5′-TCATATTTGGCAGGTTTTT CT-3′	418